



Age- and caste-independent piRNAs in the germline and miRNA profiles linked to caste and fecundity in the ant *Temnothorax rugatulus*

Ann-Sophie Seistrup^{1,2} | Marina Choppin³ | Shamitha Govind^{1,2} | Barbara Feldmeyer⁴  |
 Marion Kever³ | Emil Karaulanov¹ | Alice Séguret⁵ | Sivarajan Karunanithi¹ |
 Miguel V. Almeida^{1,6} | René F. Ketting^{1,7} | Susanne Foitzik³ 

¹Institute of Molecular Biology, Mainz, Germany

²International PhD Programme on Gene Regulation, Epigenetics & Genome Stability, Mainz, Germany

³Institute of Organismic and Molecular Evolution, Johannes Gutenberg University Mainz, Mainz, Germany

⁴Senckenberg Biodiversity and Climate Research Centre (SBIK-F), Molecular Ecology, Frankfurt, Germany

⁵School of Biological Sciences, University of Bristol, Bristol, UK

⁶Department of Biochemistry, University of Cambridge, Cambridge, UK

⁷Institute of Developmental Biology and Neurobiology, Johannes Gutenberg University Mainz, Mainz, Germany

Correspondence

René F. Ketting, Institute of Molecular Biology, Mainz, Germany.
 Email: r.ketting@imb-mainz.de

Susanne Foitzik, Institute of Organismic and Molecular Evolution, Johannes Gutenberg University Mainz, Germany
 Email: foitzik@uni-mainz.de

Funding information

Deutsche Forschungsgemeinschaft, Grant/Award Number: GRK2526/1 - Projectnr. 407023052

Handling Editor: Jacob A. Russell

Abstract

Social insects are models for studies of phenotypic plasticity. Ant queens and workers vary in fecundity and lifespan, which are enhanced and extended in queens. Yet, the regulatory mechanisms underlying this variation are not well understood. Ant queens live and reproduce for years, so that they need to protect their germline from transposable element (TE) activity, which may be redundant in short-lived, often sterile workers. We analysed the expression of two protective classes of small RNAs, microRNAs (miRNAs) and Piwi-interacting RNAs (piRNAs), in various tissues, castes and age classes of the ant *Temnothorax rugatulus*. In queens, piRNAs were highly abundant in ovaries with TEs being their clear targets, with reduced but still detectable piRNA-specific ping-pong signatures in thorax and brains. piRNA pathway activity varied little with age in queens. Moreover, the reduced ovaries of workers also exhibited similar piRNA activity and this not only in young, fertile workers, but also in older foragers with regressed ovaries. Therefore, these ants protect their germline through piRNA activity, regardless of ovarian development, age or caste, even in sterile workers often considered the soma of the *superorganism*. Our tissue-specific miRNA analysis detected the expression of 304 miRNAs, of which 105 were expressed in all tissues, 10 enriched in the brain, three in the thorax, whereas 83 were ovarian-specific. We identified ovarian miRNAs whose expression was related to caste, fecundity and age, and which likely regulate group-specific gene expression. sRNA shifts in young- to middle-aged queens were minor, suggesting delayed senescence in this reproductive caste.

KEYWORDS

ageing, castes, gene regulation, miRNAs, social insects, transposable elements

This is an open access article under the terms of the [Creative Commons Attribution](https://creativecommons.org/licenses/by/4.0/) License, which permits use, distribution and reproduction in any medium, provided the original work is properly cited.

© 2023 The Authors. *Molecular Ecology* published by John Wiley & Sons Ltd.

1 | INTRODUCTION

The origin of eusociality is considered one of the major transitions in evolution (Szathmáry & Smith, 1995). Insect societies show a high level of complexity; their colonies have been described as superorganisms (Boomsma & Gawne, 2018; Wheeler, 1911), in which the queen functions as the germline and the workers represent the soma. In ant colonies, for example, queens and workers are closely adapted to their specific roles. Ant queens focus on reproductive activity and are exceptionally long-lived, particularly in single queen societies (Keller & Genoud, 1997), wherein some queen ants can live for more than 20 years. In contrast, the typically sterile workers show high behavioural complexity performing all other tasks in the colony, including foraging and brood care. Relative to the queen, the average worker lifespan is considerably shorter, with most workers living less than a year. The different castes of social insects have been long regarded as models of phenotypic plasticity, as they are usually not genetically determined but arise due to differential transcriptional activity in the larval phase (Corona et al., 2016). While a strong investment in reproduction shortens the lifespan in many organisms (Flatt, 2011; Maklakov & Chapman, 2019), insect queens can maintain—especially in comparison to workers—a high fertility and long lifespan. Indeed, fecundity has been shown to be positively linked to a long lifespan in ants, even within a caste (Heinze & Schrempf, 2012; Negróni et al., 2020).

Our previous studies investigated the molecular regulation of ageing and fecundity in the small Myrmicine ant *Temnothorax rugatulus*, in which queens can reach lifespans of two decades. We saw that an increase in queen fecundity results in an upregulation of longevity pathways such as DNA repair and autophagy (Negróni et al., 2021). Moreover, workers that developed their ovaries upon queen removal showed an extended lifespan and transcriptional shifts in TOR and insulin-like/IGF-1 signalling (Choppin et al., 2021; Negróni et al., 2020, 2021). Gene expression shifts with age and fecundity in ant queens as well, with middle-aged queens investing more in antioxidants, but less in immunity and starvation resistance, compared to less fertile, young founding queens (Negróni et al., 2019). Although we have gained insights into the molecular pathways of ageing and fecundity in this ant and its different castes, we know little about the regulatory mechanisms underlying these shifts. All that has been shown is that histone acetyltransferase activity plays a role in the molecular regulation of ovarian development in workers in the absence of the queen (Choppin et al., 2021). We also do not know how the transcriptional differences between the castes, which lead to these divergent phenotypes, arise and are maintained.

In many social hymenopterans, workers can develop their ovaries and lay male-destined haploid eggs, a phenomenon known as arrhenotokous reproduction (Bourke, 1988). This occurs in response to specific social conditions, specifically when the queen dies or is lost. Indeed, the development and expression of reproductive traits in worker ants are socially regulated, which ensures the maintenance of the reproductive division of labour within the colony. In the ant *T. rugatulus*, workers start fighting over dominance within hours and

activate their ovaries within weeks of queen loss. These workers do not only exhibit activated ovaries but also an extended lifespan and altered regulation of mTOR or insulin-like/IGF-1 signalling (Choppin et al., 2021; Negróni et al., 2020, 2021).

In this study, we aimed to describe small regulatory RNAs (sRNAs) in the ant *T. rugatulus*, and to investigate their relationship to ovarian activity, caste and age in female ants. As will be described below, different classes of sRNAs exist, most notably microRNAs (miRNAs) and Piwi-interacting RNAs (piRNAs), and their activities have been linked to germ cells and ageing. For example, the expression of miRNAs changes during ageing in many organisms associated with transcriptional shifts of genes involved in senescence and age-related diseases (Kinser & Pincus, 2020). In the honeybee *Apis mellifera*, specific miRNAs are associated with age-dependent behavioural changes (Behura & Whitfield, 2010). PiRNAs represent a class of sRNAs that is particularly active in the germline (Ketting & Cochella, 2021; Ozata et al., 2019), where they regulate the activity of transposable elements (TEs). There is also growing evidence that TE activity is a consistent molecular hallmark of ageing (Sturm et al., 2017). In the termite *M. bellicosus*, TE-associated genes are upregulated and genes from piRNA pathways are downregulated in old workers with short residual lifespans, compared to long-lived reproductives (Elsner et al., 2018). Moreover, TE expression in the fat body of the termite *Macrotermes natalensis* does not rise with increasing queen age, likely due to the protective upregulation of piRNA pathways in this reproductive caste with delayed ageing (Post et al., 2023). Similarly, in *A. mellifera*, the piRNA repertoire and expression levels are greater in reproductive individuals than in sterile workers, with the ovaries, representing the female germline, being the tissue of highest expression (Wang et al., 2017). Haploid males, in which deleterious effects of TEs dominate, exhibit the highest piRNA levels, but surprisingly also the highest TE expression. The honeybee is a TE-deficient species with TEs making up only 3% of the genome (Elsik et al., 2014; Kapheim et al., 2020). Yet, an active piRNA system is still required to protect the vulnerable haploid male genome and the reproductive castes from TE-induced genomic instability (Wang et al., 2017). Ant genomes often contain higher proportions of TEs (Gilbert et al., 2021). For example, recently published ant genomes reported values around 20%–32% (Bohn et al., 2021; Faulk, 2023; Nouhaud et al., 2022) and we estimate that 33.3% of the *T. rugatulus* genome is covered by repetitive elements.

Different classes of sRNAs exist, which all form effector complexes with proteins of the Argonaute family and typically repress gene activity (Ender & Meister, 2010). Two of the major sRNA pathways are the miRNA pathway (reviewed in Bartel, 2009) and the piRNA pathway (reviewed in Ozata et al., 2019) and we focus here on the expression of these two classes of sRNAs. miRNAs are transcribed from distinct loci and the resulting transcripts form hairpin structures, which are processed by specific nucleases to produce mature miRNAs (Bartel, 2009). After binding their respective Argonaute proteins, miRNAs direct the binding of this protein to specific mRNAs, based on base-pairing between the miRNA and the mRNA, and repress their activity (Filipowicz et al., 2008). As

miRNAs bind their target mRNAs through only partial complementary base-pairing, it can be difficult to predict which genes a certain miRNA targets, and many tools exist to tackle this (Bartel, 2009; Lewis et al., 2003). The targets of miRNAs are typically protein-coding genes that have regulatory roles themselves (Bartel, 2009).

Much like miRNAs, piRNAs are transcribed from distinct loci in the genome. However, unlike miRNAs, which can be found in any tissue, piRNAs are often restricted to the germline. This is at least true for model organisms like *Drosophila*, *Caenorhabditis elegans* and mice. However, in various arthropods, somatic piRNAs have been detected (Lewis et al., 2018) suggesting that the ancestral state of piRNA expression may have been more widespread. The processing of piRNA precursor transcripts into mature piRNAs does not proceed via a hairpin intermediate, but utilizes a different, complex molecular machinery as reviewed in Zhang et al. (2022). Mature piRNAs are bound by a specific subfamily of Argonaute proteins: Piwi proteins. Piwi-piRNA complexes are known to elicit strong silencing effects, both at the transcriptional and post-transcriptional levels (Ozata et al., 2019). When a Piwi-piRNA binds a target, it may turn the targeted mRNA into a new piRNA in a process known as the ping-pong cycle (Luo & Lu, 2017; Ozata et al., 2019), which results in sense and antisense piRNAs that overlap precisely 10 nucleotides at their 5' ends. Finally, piRNAs have a strong bias towards uracil at the 5'-position, matched by an adenine at position 10, due to the described ping-pong cycle. A deeply conserved role of piRNAs is the silencing of TEs and the protection from non-self DNA (Madhani, 2013). As a consequence, piRNA sequences are typically not conserved, even between closely related species, as they co-evolve with the TEs they control.

Here, we characterize the sRNA classes in the ant *T.rugatulus* with a focus on miRNAs and piRNAs and by using high-throughput sequencing of various castes, age classes and tissues, and determine whether sRNA profiles are tissue and/or caste specific. We also explored whether they change with age or reproductive status of the queen and worker castes.

2 | MATERIALS AND METHODS

2.1 | Ant collection and maintenance

Temnothorax rugatulus ants are widespread in western North America and live in coniferous forests, under rocks or in crevices. In August 2015 and 2018, we collected several hundred colonies in the Chiricahua Mountains (see Choppin et al., 2021; Negrone et al., 2019 for GPS information on exact locations). Collection permits for the Coronado National Forest were obtained through the Southwestern Research Station of the Museum of Natural History in Portal, Arizona. The ant colonies were transported to our laboratory in Mainz, Germany, where they were relocated to individual boxes with plastered flours containing nests made of plastic inserts between two glass plates covered with red foils to block the light. The colonies were kept in climate chambers at 18°C and 70% humidity in

a 12:12 light-dark cycle. They were fed with honey and crickets and received ad libitum water.

2.2 | Analysis of miRNA and piRNA expression depending on queen age and tissue

For our first aim of investigating differences between tissues and age of queens, we sequenced RNAs from young and old queens. Seven young queens were collected during our 2018 trip as founding queens either alone or with their first workers, invariably less than six. These queens likely had established their colony in July or August of that year, so they were less than 6 months old. Seven older queens were collected in Arizona in August 2015 in large single-queen colonies, indicating that, at the time of collection, they were likely several years old. We kept them for another 3 ½ years so that at the time of sampling, we estimate their age to be between 6 and 12 years. *Temnothorax* ant queens can live for up to 20 years (Plateaux, 1986), so our older queens were probably middle-aged when sampled. At the time of sampling, colonies of these young and older queens comprised between 60 and 230 workers. In November 2018, the queens were provided with fresh boxes, nests and food and housed in a climate chamber at 25°C and 70% humidity on a 12:12 light-dark cycle. All queens came from single-queen colonies.

After 1 month under the same conditions, the queens were dissected in ice-cold PBS under a Leica stereomicroscope. The head with the thorax and the ovaries were removed from each queen, separately frozen in liquid nitrogen and stored at -80°C. We measured ovariole length and counted the number of white eggs (i.e. eggs in development) in the ovaries using the Leica software LAS v4.5. One young queen had died before the dissection date and was therefore not sampled. Differences between old and young queens were assessed using R v.4.3.1. For the number of eggs, we used a generalized linear model ($\text{glm}(\text{eggs} \sim \text{age}, \text{family} = \text{quasipoisson})$), and for the lengths, we used a linear model ($\text{lm}(\text{length} \sim \text{age})$).

In August 2020, the brains of the queens were isolated from their heads on ice, placed in 50 µL TRIzol™ (Life Technologies), frozen in liquid nitrogen and stored at -80°C. The brain of one young queen was not removed because her head was damaged. The brain was placed in 50 µL TRIzol, frozen in liquid nitrogen and also stored at -80°C. Two weeks later, the RNA was extracted from the brain and thorax samples. For this, 50 µL chloroform was added to the samples, the tubes were swirled and placed on normal ice for 5 min. The samples were then centrifuged at 12000×g and 4°C for 15 min. The resulting upper phases were transferred to new 1.5 mL Eppendorf tubes using gel loading tips. Then, 25 µL of 100% ethanol was added to the upper phases, the tubes were swirled and the samples were transferred to Zymo-Spin IC columns (Direct-zol RNA Microprep Kit from Zymo Research) in collection tubes. The collection tubes containing the columns were centrifuged at 12000×g for 30 s at room temperature, and the columns were then transferred to new collection tubes. 400 µL RNA wash buffer was added to the columns, which were then centrifuged at 12000×g for 30 s at room temperature.

5 μ L DNase I was carefully mixed with 35 μ L DNA digestion buffer and added to the columns. The samples were incubated for 15 minutes at room temperature. Then, 400 μ L Direct-zol PreWash was added to the columns and they were centrifuged at 12000 \times g for 30s at room temperature. The residues were discarded, and the previous step was repeated. 700 μ L of RNA wash buffer was added to the columns, which were then centrifuged at 12000 \times g for 1min at room temperature. The columns were transferred to RNase-free tubes and 15 μ L of DNase/RNase-free water was added directly to the column matrices. Finally, the collection tubes containing the columns were centrifuged at 12000 \times g for 30s at room temperature to elute the RNA and the columns were discarded. The RNA samples were stored at -80°C until sequencing. In November 2020, 50 μ L of ice-cold TRIzol was added to the ovary samples and the RNA was extracted using the same procedure as described above.

2.3 | Analysis of miRNA and piRNA expression in ovarian tissue of queens and workers

For our second aim of comparing queens to workers of different fertility stages, we sequenced RNA from queens and workers either from colonies with a queen (queenright, ql) or from colonies lacking a queen (queenless, q). *T. rugatulus* female ants display a gradient in terms of reproductive potential and life expectancy. Both traits are most pronounced in the queen; only she can mate, and her ovaries also possess a spermatheca and eight ovarioles. Worker ovaries are smaller and are composed of only two ovarioles. Fertile nurses in ql colonies are the longest lived and most fertile individuals after the queen. They are followed by the nurses from qr colonies and finally by the old foragers from these colonies. This gradient allows us to analyse at which point these female ants stop protecting their germline from TEs or whether germline tissue always expresses Piwi protection.

At the end of 2021, 12 qr and 12 ql colonies with between 20 and 100 workers were provided with fresh boxes, nests and food and housed in a climate chamber at 25°C and 70% humidity on a 12:12 light:dark cycle. We aimed to sample four independent replicates of each of the four groups: queens, qr nurses (qr-n) and foragers (qr-f) and ql nurses (ql-n). After 1 month, in January 2022, we dissected the ovaries of the queen, four nurses and five foragers from 12 qr colonies each, and the ovaries of four nurses from 12 ql colonies. For each queen replicate, the ovaries of three queens from three different colonies were pooled. For each nurse replicate (qr and ql alike), we pooled the ovaries of four workers from three colonies, with no overlap between replicates, for a total of 12 ovaries. For the forager replicates, we pooled the ovaries of five foragers from three colonies, for a total of 15 ovaries each. We have pooled 15 ovaries from foragers to get enough material, as foragers are known to have the most regressed ovaries, as we show below. Dissections were conducted in ice-cold PBS under a stereomicroscope and ovaries were photographed using the Leica system LAS v4.5. We noted the number of eggs in development and grouped the ovaries of queens and workers into five developmental stages (0=regressed ovaries:

thin, clear tubes; 1=undeveloped ovaries with rounded tubes and a wider end, 2=slightly developed ovaries containing immature eggs; 3=developed ovaries with one mature egg, 4=well-developed ovaries with 2-5 mature eggs, 5=extremely well-developed ovaries with >5 eggs). Dissections took less than 5 minutes and ovaries were transferred into 100 μ L Trizol, which was kept on ice until all ovaries of one pooled sample were added and then stored at -80°C . Differences between groups were assessed using R v.4.3.1. For the number of eggs, we used a generalized linear mixed effects model (glmer(eggs ~ group + (1|Colony), family=poisson). Due to a singularity in the model, we could not include colony ID in the analyses of developmental stages and instead performed a glm (glm(stage ~ group, family=poisson)).

Each sample was ground while frozen and then RNA was extracted with the Direct-zol RNA Microprep kit following the standard instructions. RNA was resolved in 15 μ L RNase/DNase-free water and stored at -80°C before sequencing.

2.4 | Sequencing

NGS library prep was performed with NEXTflex Small RNA-Seq Kit V3 following Step A to Step G of Bio Scientific's standard protocol (V19.01) using the NEXTflex 3' SR Adaptor and 5' SR Adaptor

(5'rApp/NNNNTGGAATTCTCGGGTGCCAAGG/3ddC/and 5'GUUCAGAGUUCUACAGUCCGACGAUCNNNN, respectively). Libraries were prepared with a starting amount of 5 ng and amplified in 21 PCR cycles (1st data set, different tissues of old and young queens), or a starting amount of 1.5ng and amplified in 22 PCR cycles (2nd data set; ovaries of different castes). Note that we do not directly compare these two different data sets, such that this difference in PCR cycle number does not affect our conclusions. Amplified libraries were purified by running an 8% TBE gel and size selected for 15–40nt. Libraries were profiled in a high sensitivity DNA Chip on a 2100 bioanalyser (Agilent Technologies) and quantified using the Qubit dsDNA HS Assay Kit, in a Qubit 2.0 fluorometer (Life Technologies). All samples were pooled in equimolar ratio and sequenced on 1 high-output NextSeq 500/550 flow cell, SR for 1x 84 cycles plus 7 cycles for the index read.

2.5 | Read preprocessing, mapping and filtering

NGS library quality was assessed using FastQC v0.11.8 (Andrews, 2010) before removing the constant sequence of the 3'-NextFlex adapter using Cutadapt v2.4 (Martin, 2011) (-a TGGAA TTCTCGGGTGCCAAGG -m 26 -M 43). Trimmed libraries were once again assessed for quality using FastQC. Reads were mapped to the draft genome assembly 'trug_v1.0' (BioProject PRJNA750352, in submission) using Bowtie v1.2.2 (Langmead et al., 2009) allowing for one mismatch and reporting one best alignment in cases of multimapping while concomitantly removing the random 2x 4nt random NextFlex adapter bases (bowtie -p 16 -v 1 -M 1 -y --best

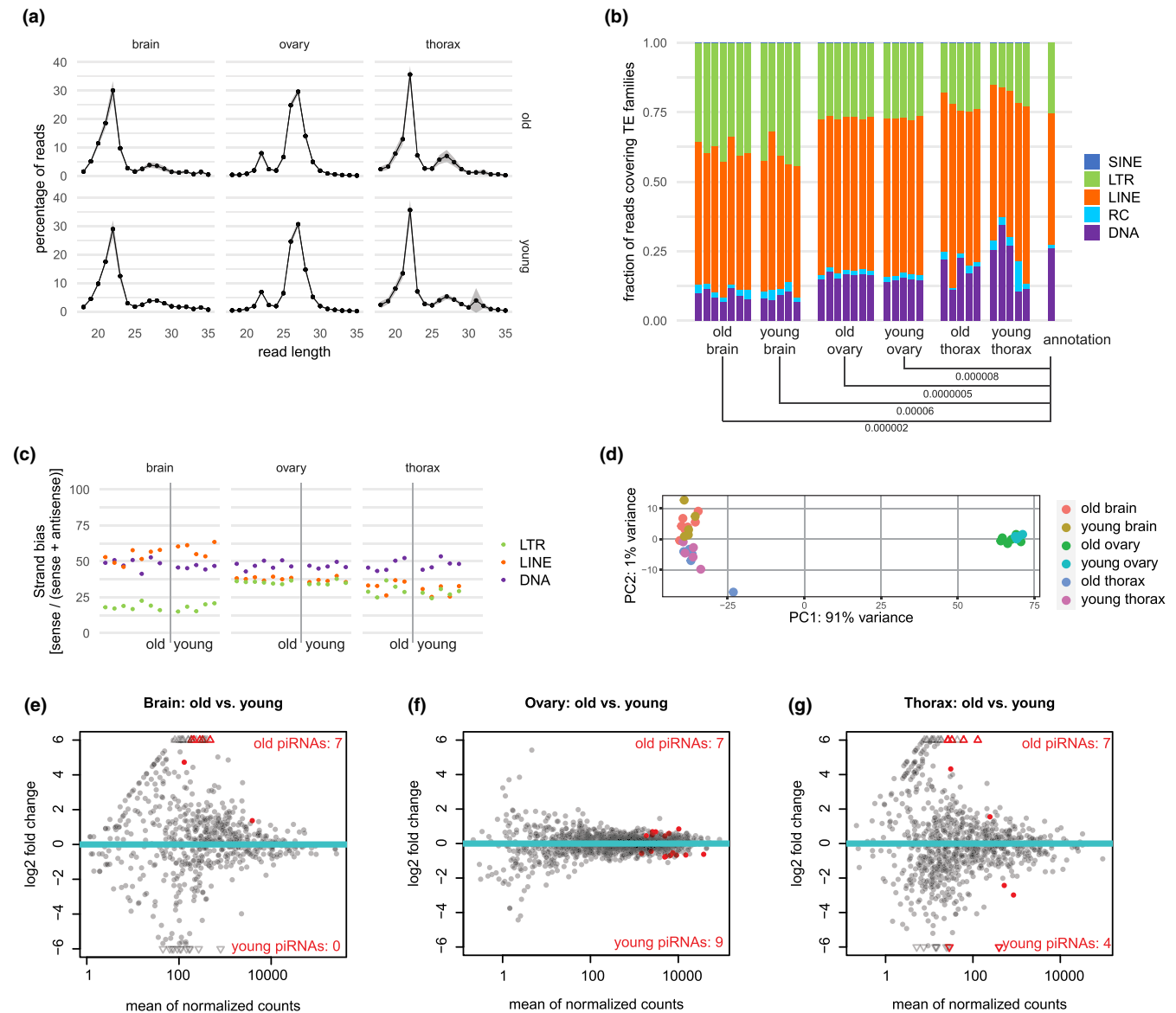


FIGURE 1 piRNA expression in different tissues of young- and middle-aged queens. (a) Length distribution of 18–35 nt reads generated by sRNA-Seq. Shaded areas depict standard deviation, obtained from the five to seven biological replicates. (b) Stacked bar plots showing piRNA-like reads (25–30 nt) covering different TE families. *T*-tests carried out for each TE family to find difference between old and young and between each group and annotation (random expectation). For each pair of comparisons, the lowest Holm-adjusted *p*-value is shown, if this is significant ($p < .05$). All values not shown are listed in the supplementary data. (c) Strand bias (%) of piRNA-like reads derived from LTR, LINE and DNA elements in the three tissues, obtained from young and older queens ($n = 5-7$). (d) Principal component (PC) analysis of piRNA-like reads (25–30 nt) that map to annotated TEs. (e–g) MA plots showing the pairwise differential TE comparisons of piRNA targeting in young versus older queens in the three tissues. Each dot represents one TE type and red indicates significant changes ($FDR < 0.05$). All hits are reported in [Table S1](#).

--strata --trim5 4 --trim3 4). Read lengths were assessed by a custom Python script (<https://github.com/Tunphie/SequencingTools/blob/main/summarizeNucleotideByReadLength.py>) and plotted using ggplot2 (Wickham, 2016) in R v3.13 (R Core Team, 2013). Based on the length profiles as shown in [Figure 1a](#), mapped reads were subsequently split into different lengths for further analysis of piRNAs (reads of length 25–30 nt) and miRNAs (reads of length 18–24 nt) using samtools v1.9 (Daneczek et al., 2021) and GNU awk. These mapped reads were further split into non-overlapping and overlapping reads with miRNA or transposon annotation in sense or

antisense orientation using the function intersectBed from bedtools v2.27 (Quinlan & Hall, 2010). This was done in order to determine lengths and 5'-biases using the aforementioned Python script before plotting these with ggplot2 in R.

2.6 | piRNA analyses

Reads in the piRNA-range (25–30 nt) existing outside of our annotated transposons were split into plus and minus strand using

samtools v1.9. BigWig files were then generated for each strand separately using the deepTools v3.5.1 (Ramírez et al., 2016) function bamCoverage. Means of groups were calculated using WiggleTools (Zerbino et al., 2014) and converted back into BigWig files using wigToBigWig from UCSC. The tools computeMatrix and plotProfile from deepTools v3.5.1 were used to generate views of the mapped data coverage over selected loci provided as a BED file.

Reads in the piRNA-range (25–30nt) overlapping with our annotated transposons (supplementary file TE_Annotation.trug.fa.out.gv; courtesy of Jongepier et al. (2022)) were counted using Subread v2.0.0 (Liao et al., 2013) (featureCounts -s 0 -M -F SAF), thereby summarizing read counts per transposon of the same type ($n = 1903$). For strand-bias analysis, featureCounts was used with parameter '-s 1' for TE-sense and '-s 2' for TE-antisense read counting. The provided annotation contain TEs covering 27.1% of the *T. rugatulus* genome, defined from an initial 33.3% repetitive elements found by use of RepeatMasker (v4.0.8; Smit et al., 2013–2015). Reads in different transposon families were subsequently summarized in R by comparison to the used annotation file. T-tests and subsequent Holm-correction for multiple testing were carried out in R. Differential analyses were carried out using DESeq2 v1.30.1 (Love et al., 2014) in R v4.0.3. A false discovery rate (FDR) or 0.05 was used without a fold-change cut-off. PCA plots and MA plots were generated using plotPCA and plotMA from the DESeq2 package.

Samples were randomly downsized to 500K (old and young queens; thorax, brain and ovaries) or 2 million (ovaries of queens, nurses and foragers) reads per sample for our two data sets, respectively, using first samtools collate and then shuf (-n 500,000/-n 2,000,000). These reads were then used to search for ping-pong signatures using PingPongPro v1.0 (Uhrig & Klein, 2019, -p -v -o). Ping-pong pairs were compared to the TE annotation and divided into signatures existing within TEs and outside of TEs using R. PingPongPro was further run using the TE annotation as input, and mapping relative to TE families was counted using R. Plots were generated using ggplot2 in R. UpSet plots were generated using UpSetR (Conway et al., 2017).

2.7 | miRNA prediction and annotation

We used miRDeep v2.0.1.3 (Friedländer et al., 2012) on reads of length 18–24 nt to predict miRNA de novo. We first used mapper.pl script (-d -e -h -i -j -m -o 30 -v -p -s -t) to process the reads and map them to our partial *T. rugatulus* genome. The outputs from mapper.pl along with our partial genome and miRNA annotations of four insect species (*A. mellifera*, *D. melanogaster*, *T. castaneum* and *B. mori*) from miRBase v22 were used to predict miRNAs using the miRDeep2.pl script (-g 100,000 -P). We quantified the predicted miRNAs using the quantifier.pl (-d) script. Furthermore, we removed predicted miRNAs that did not satisfy the following quality filters adapted from Coenen-Stass et al. (2018). The miRNAs should (i) have a miR-Deep2 score above 1, (ii) have a statistically significant miRDeep2 randfold p -value ($p < 0.05$), (iii) have a sequence that does not match any tRNAs or rRNAs in RFAM (Griffiths-Jones et al., 2003) and (iv) have at least one read in three or more of our samples from our

first data set (old and young queens; thorax, brain and ovaries). The predicted miRNAs were stringently annotated by miRDeep2 looking for exact seed match in the four insect species. Additional low-confidence annotation was made by blasting the sequences of the miRNAs of interest against a broad category of known hexapod miRNAs from miRBase using blast v2.10.1 with relaxed parameters (-evalue 20 -word_size 4 -reward 5 -penalty -4 -gapopen 25 -gapextend 10 -num_threads 10 -max_target_seqs 1 -outfmt 6). The specific software parameters used are mentioned in parentheses following the respective scripts.

2.8 | miRNA analyses

Reads in the miRNA-range (18–24 nt) aligning to our miRNA annotation (mature sequences) were counted using Subread v2.0.0 (featureCounts -s 1 -M -F SAF --minOverlap 18). miRNA expression for a given tissue (brain, ovary and thorax) was defined as non-zero read counts in at least three samples from that tissue regardless of age. This number was chosen arbitrarily, as choosing two or four samples yielded almost the same results (115 or 96 miRNAs, respectively, instead of the 105 we now report). Overlap of these reads were plotted using VennDiagram in R (Chen & Boutros, 2011). Differential analyses were carried out using DESeq2 v1.30.1 in R v4.0.3. A false discovery rate (FDR) of 0.05 was used without a fold-change cut-off. PCA plots and MA plots were generated using plotPCA and plotMA from the DESeq2 package.

We note that some of our reads may be misclassified; either as the wrong sRNA type or as a sRNA when it was indeed the breakdown product of a functional RNA (Ludwig et al., 2017). Some piRNAs might also have been breakdown product of rRNAs (Figure 3d,f,g and Figure S2d). A few non-TE-derived piRNA reads resembled structural reads (Figure S1–S2d). Also some piRNAs may have been misclassified as miRNAs due to the closeness of their length distributions and their similar 5'-bias. We do, however, believe that most piRNAs would be filtered out of our differential miRNA analyses since these are the only reads mapping sense to our miRNA annotation. We also are aware that sRNA populations other than miRNAs and piRNAs exist, and that some of our sRNAs may have been misclassified due to not investigating further sRNA families such as small interfering RNAs (siRNAs).

3 | RESULTS

3.1 | Basic sRNA profiling of three *T. rugatulus* tissues

In order to investigate tissue-specific expression of sRNAs in *T. rugatulus*, we sequenced sRNAs of 15–40 nucleotides (nt) from the thorax, ovaries and brain of young, founding queens below 6 months of age and middle-aged established queens above 3.5 years. When comparing the read length distribution, two distinct populations

were observed; one in the typical miRNA range (18–24 nt) and one in the piRNA range (25–30 nt; Figure 1a). The peak in the piRNA range was more prominent in the ovaries than in the somatic tissues, consistent with findings in other animals of high piRNA pathway activity in the germline. In contrast, the miRNA-range peak was more prominent in the somatic tissues, although a distinct piRNA-range peak could still be observed in these tissues (Figure 1a). To probe deeper into the characteristics of the sRNA molecules, we aligned the reads to a genome assembly from Jongepier et al. (2022). A large fraction of the reads mapped to multiple locations in the genome (Figure S1–S2a), which could mean that these map to repetitive elements such as TEs. Below, we will describe the miRNA- and piRNA-range sRNAs in soma and germline in separate sections. Lastly, comparisons between young- and middle-aged queens will be described.

3.2 | Queen ovaries express TE-targeting piRNAs

After having determined that ovaries have a prominent piRNA-like sRNA population, which peaked at abundance at lengths of ~26–28 nt, we extracted all reads in the range 25–30 nt and compared these to a TE annotation provided by Jongepier et al. (2022), since piRNAs are known to be involved in TE repression, particularly in gametes. We saw that many reads, up to 60%, overlapped with annotated TEs in the queen ovaries (Figure S1–S2b). We further extracted these TE-derived reads and saw that they mapped to both sense and antisense strands of TEs, with some bias for the antisense strands, as has been previously shown for piRNAs in other species (Figure S1–S2c). The reads furthermore had a strong bias for U at the 5'-position, another common feature of piRNAs (Figure S1–S2c). Compared to the genome-wide TE annotation, DNA and rolling circle-derived piRNAs were slightly underrepresented in the piRNA-like reads in the ovaries, whereas LTR- and LINE-derived reads were mildly overrepresented (Figure 1b).

In the absence of available gene annotation, we could not determine where the piRNA-like reads, that were not assigned to TEs, mapped. Nevertheless, the reads mapping outside of TEs also had a 5'-U bias and showed mapping on both genomic strands similar to the TE-derived sRNAs (Figure S1–S2d) with at least some of the sense/antisense reads stemming from the same genomic position (Figure 1e). We noticed that some loci were strongly biased to produce sRNAs from only one of the strands (Figure S1–S2e), suggesting that these may not be true piRNAs. Alternatively, these may represent highly strand-biased populations of piRNAs (Brennecke et al., 2007; Hirano et al., 2014).

Taken together, the above results are consistent with the idea that this 25–30 nt sRNA population corresponds to piRNAs. To further assess this, we probed for so-called ping-pong signatures, which arise when cleaved piRNA target transcripts are themselves turned into piRNAs. Such piRNAs will display a characteristic 10 nt overlap on their 5' end with the piRNA that induced the cleavage. We first downsampled all data sets of 25–30 nt reads to 500K reads in order

to enable comparison between them, and then searched for possible ping-pong signatures using PingPongPro (Uhrig & Klein, 2019). We found around 4000 high-fidelity ping-pong pairs in the ovaries across the entire genome, around two-thirds of which were found inside annotated TEs (Figure S1–S2f). We then looked for ping-pong pairs specifically in the TEs and noticed that the majority of them were derived from LTR and LINE elements with more than 50% of TE-derived ping-pong signatures stemming from LTR elements (Figure S1–S2g). Given that LTR elements only amount to 25% of the annotated transposons, this represents a significant overrepresentation and suggests that these TE types are most actively targeted by the Piwi pathway. In the absence of functional antibodies, which would allow us to test whether the identified sRNAs are bound to Piwi proteins, we conclude that the reported sRNA species represent piRNAs, and that *T. rugatulus* ovaries express an active piRNA pathway, with LTR retrotransposons as important targets.

3.3 | Thorax and brain have limited piRNA expression in queens

Next, we probed the queens' thorax and brain samples for the existence of piRNAs. In both tissues, we did find a population of small RNAs that displayed similar features as the piRNAs in the ovaries with length peaks at roughly 27 nt (Figure 1a). They showed a mild bias towards antisense polarity with respect to their matching transposons, and they displayed a strong bias for a 5'-U (Figure S1–S2c). Interestingly, the brain had more piRNAs mapping outside of annotated TEs (Figure S1–S2b,d,e), possibly pointing towards a function of piRNAs other than transposon surveillance.

In contrast to ovaries, ping-pong signatures were practically absent in the brain (0–200 signatures per 500K reads per sample). Some high-fidelity ping-pong signatures, around 500 per 500K reads (overall average: 459, average in old samples: 572, average in young samples: 346), were found in the thorax (Figure S1–S2f), but their abundance was still roughly 5- to 10-fold lower compared to ovaries. Ping-pong results were not strongly affected by age (Figure S1–S2f).

Then, we checked how the available piRNAs were distributed over the different TE families. In the thorax, the piRNAs were distributed along the annotated transposons roughly according to their representation in the genome, albeit with high variance between samples (Figure 1b). Interestingly, the brain samples showed a consistent overrepresentation of LTR elements relative to DNA elements (Figure 1b). These results could point to differential activities of TE families in these two tissues.

We noticed that the strand bias of LTR and LINE elements differed in the brain relative to the ovaries and thorax (Figure 1c): LTR-derived piRNAs showed a much more extreme anti-sense bias, whereas LINE-derived populations showed a weaker anti-sense bias and even a mild over-representation of sense piRNAs. These findings may also reflect differential TE activities in the brain compared to the thorax and ovaries.

3.4 | piRNA expression shifts only minimally with queen age

We saw no difference in TE family targeting or strand bias between young- and middle-aged queens (Figure 1b,c). In order to further determine whether ageing of *T. rugatulus* queens is associated with differential targeting of specific TEs by piRNAs, we carried out differential analyses of this subset of sRNAs using DESeq2 (Love et al., 2014). piRNAs found to be differentially expressed between young and older queens in different tissues are provided in Table S1.

The principal component analysis revealed that the largest differences in piRNA expression existed between ovarian and somatic tissues, irrespective of age (Figure 1d). Nevertheless, we investigated further the effects of age in all three tissues. In the ovaries, we detected 16 differentially targeted transposons, 7 of which were Penelope elements. The differential abundance was, however, minor (Figure 1f). The piRNA profiles of thorax and brain were noisier, but we were able to define 11 and 7 differentially targeted transposons respectively (Figure 1e,g). In the thorax, much like in the ovaries, these were mainly Penelope elements (6/11), whereas the transposons significantly affected in the brain were mainly targeted by lowly expressed piRNAs (Figure 1e). We conclude that piRNA expression changes only marginally with age in *T. rugatulus* queens.

3.5 | Foragers have less developed ovaries than nurses and queens

The weak differences in piRNA expression between young- and middle-aged queens led us to determine their fecundity, thinking that low fertility and loss of ovarian piRNA expression might be associated. The ovaries of young- and middle-aged queens did not differ in the number of eggs in development (glm (quasipoisson): $df=1$; $\chi^2=1.54$; $p=.21$, Figure 2a), nor in ovariole length (lm(length~age), Figure 2b). In contrast, we found strong differences in egg production and ovarian development between the different groups of queens and workers, when we dissected the ovaries of four different groups; queens, nurses and foragers from colonies with a queen (queenright, qr) and nurses from colonies lacking a queen (queenless, ql). Queens had more eggs than all worker types, while foragers had fewer eggs in development than nurses (glmer(family=poisson + (1|Colony)): $df=3$; $\chi^2=427.03$; $p<2.2e-16$; queen - ql-nurse: $p<.001$; queen - qr-forager: $p<.001$; queen - qr-nurse: $p<.001$; qr-forager - ql-nurse: $p<.001$; ql-nurse - qr-nurse: $p=.79$; qr-nurse - qr-forager: $p<.001$, Figure 2c). We further defined the developmental stage of the ovaries ranging from 0 (undeveloped; no eggs in development) to 5 meaning (fully developed; more than five eggs in development) (Figure 2d). Here, we could also see that queens had much more developed ovaries than any worker type, while nurses generally had more developed ovaries than foragers (glmer (family=poisson): $df=3$; $\chi^2=72.483$; $p=1.255e-15$; queen - ql-nurse: $p<.003$; queen - qr-forager: $p<.001$; queen - qr-nurse: $p<.001$; qr-forager - ql-nurse: $p<.001$; ql-nurse - qr-nurse: $p=.68$; qr-nurse

- qr-forager: $p<.001$, Figure 2e). We were surprised to observe that there were no significant differences between the ovarian developmental stages of nurses from qr and ql colonies (Figure 2c,e), though workers from ql colonies were shown to undergo ovarian activation (Choppin et al., 2021; Negroni et al., 2020, 2021).

3.6 | piRNAs are expressed in the ovaries of queens and all worker types

After having determined that, in queens, piRNAs act primarily in the ovaries, we sought to investigate the piRNA profiles of ovaries from workers, even if they are only present as almost rudimentary organs. To allow proper comparison, we again sequenced sRNAs from the ovaries of queens, but this time also included the ovaries of foragers and nurses from qr colonies as well as nurses from ql colonies, where activation of the nurses' ovaries is triggered. Analysing these four different groups allowed us to investigate differences in caste, worker task and conditional changes to nurses. Surprisingly, we obtained near-similar piRNA expression profiles in the ovaries of all four groups (Figure 3a and Figure S2a) and only a slight depletion of ping-pong signatures in worker ovaries (Figure S2b). Multimapping reads were again abundant in all samples (Figure S2c). As previously seen for the different queen tissues (Figure 1b), TE family targeting did not differ between these different groups. Relative to the distribution of all annotated TEs, all samples showed a bias towards LINE elements at the expense of DNA elements (Figure 3b).

We carried out a differential analysis of our defined piRNAs using DESeq2 and observed only minor differences between the different groups, reflected in the clustering in the principal component analysis (Table S2, Figure 3c). Nonetheless, we could define several TEs with differential piRNA expression between groups with a particular upregulation of piRNAs in queens compared to foragers (Figure 3d-i). In general, those TEs that were found to be differentially targeted were those for which piRNAs were generally more abundant (Figure 3d-h), suggesting that, although the general upregulation of piRNAs in active versus inactive ovaries is modest (Figure 3a), the effect likely is biologically relevant.

We found one TE to be highly upregulated in foragers in several analyses (Figure 3d,f,g), namely the Copia element. However, when further investigating the various Copia loci, we noticed that only one peak existed in each locus and that it consisted of only sense reads with no ping-pong signatures. We therefore extracted the sequences in the peaks and saw that these all aligned not only to each other but also to the 3' end of large subunit rRNA from *Bombus affinis* (Figure S2d). Given the strong homologies of rRNA sequences between species, we anticipate that this potential Copia-derived piRNA is not a genuine piRNA but rather an rRNA fragment that was relatively higher expressed in the foragers as a result of their slightly lower piRNA expression. This finding indicates that effects on individual TEs need to be treated with care. Therefore, we restricted our analyses to overall patterns and did not investigate individual loci. We conclude that piRNAs are similarly active in the ovaries of

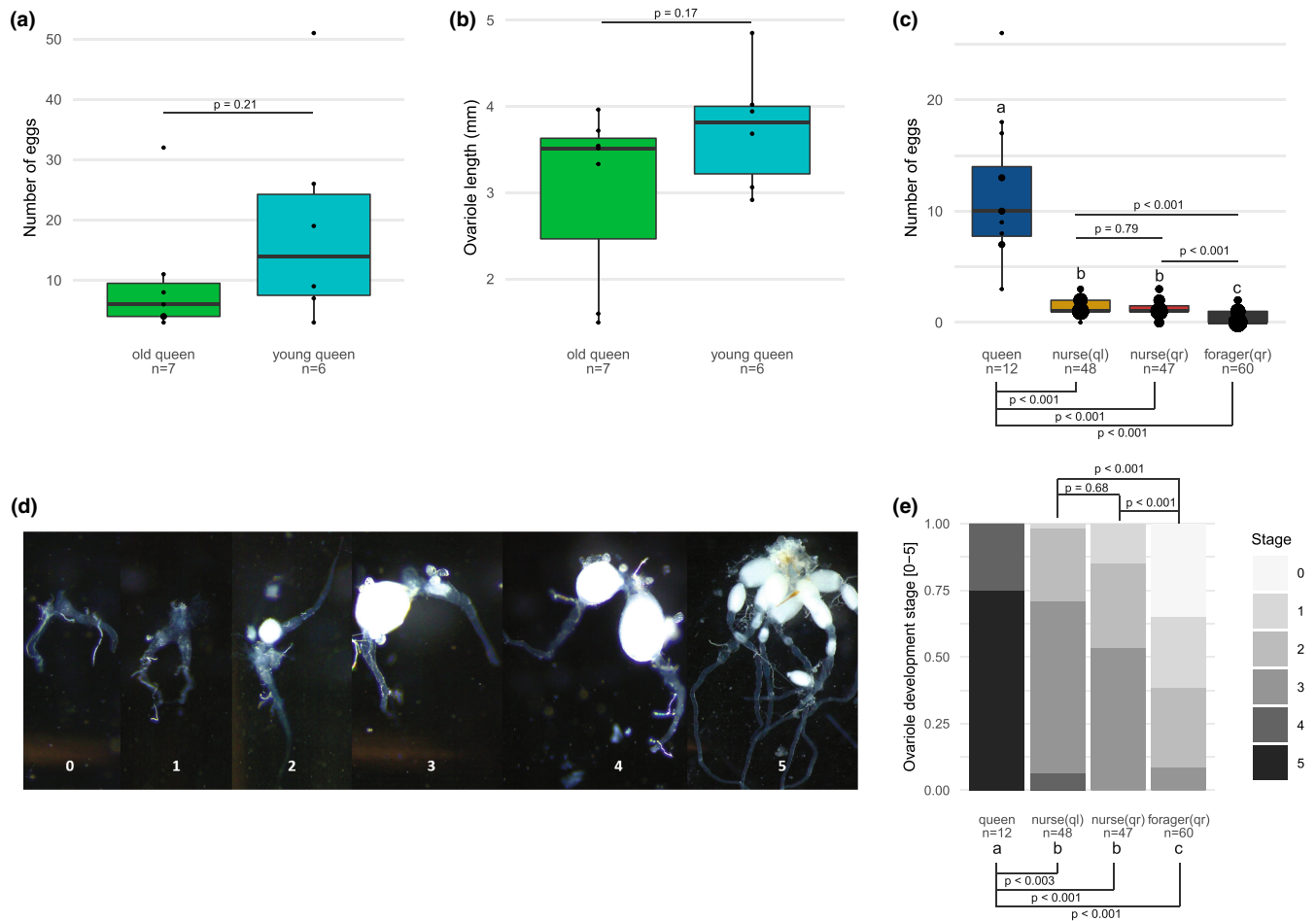


FIGURE 2 Fecundity of *T. rugatulus* queens and workers of different ages and status as determined by ovarian development and egg production. (a) Boxplots of the number of eggs in development found in the ovaries of young, founding queens (<6 months old) and middle-aged established queens (>3.5 years old). *p*-value for general linear model (quasipoisson) indicated. (b) Boxplot of ovariole lengths of young and older queens. Point size is relative to number of replicates. *p*-value for linear model indicated. (c) Boxplots of the number of eggs in development found in queens, nurses and foragers of qr colonies and nurse workers of ql colonies. Point size is relative to number of replicates. *p*-values for generalized linear mixed-effects model (family = poisson + (1|Colony)) indicated, letters indicate significance. (d) Representative pictures of five defined developmental stages of ovaries. 0 = regressed ovaries: thin, clear tubes; 1 = undeveloped ovaries with rounded tubes and a wider end, 2 = slightly developed ovaries containing immature eggs; 3 = developed ovaries with one mature egg, 4 = well-developed ovaries with two to five mature eggs, 5 = extremely well-developed ovaries with >5 eggs. (e) Boxplot of the distribution of each caste into the five developmental stages as defined in (d). *p*-values for generalized linear mixed-effects model (family = poisson) indicated, letters indicate significance. qr, queenright, ql, ueenless.

all female castes, with only marginal upregulation of already heavily targeted TEs in fully active ovaries. We also infer that piRNAs are unlikely directly involved in the activation of ovaries in nurses upon removal of the queen.

3.7 | *T. rugatulus* miRNAs

We then investigated miRNA-like reads. First, we used miRDeep2 (Friedländer et al., 2012) to carry out a de novo miRNA prediction in our draft genome using miRNAs from four related species (*Bombyx mori*, *Drosophila melanogaster*, *Apis mellifera* and *Tribolium castaneum*) as a reference and the pooled small RNA-seq data of all samples. Thereby, we could detect 1191 possible miRNAs. We

then filtered these putative miRNAs using four parameters (see Methods) to ensure high fidelity of our generated miRNA annotation. After filtering, we were left with 372 miRNA loci coding for 304 distinct miRNAs (Table S3). Most of the miRNAs were unique, that is, only found at one locus, and no miRNA was present at more than five loci. Notably, the identified miRNAs included strongly conserved miRNAs such as let-7 and mir-9 known to be ubiquitously expressed in other species.

After having generated our reference, we overlapped this with our mapped reads in the range 18–24 nt from young and older queens. We saw that the reads mainly mapped sense to our defined miRNA loci, as would be expected for miRNAs (Figure 4a). We could further show that *T. rugatulus* miRNAs have a strong 5'-U bias (Figure 4a). A strong bias for 5'-U has also been indicated in other

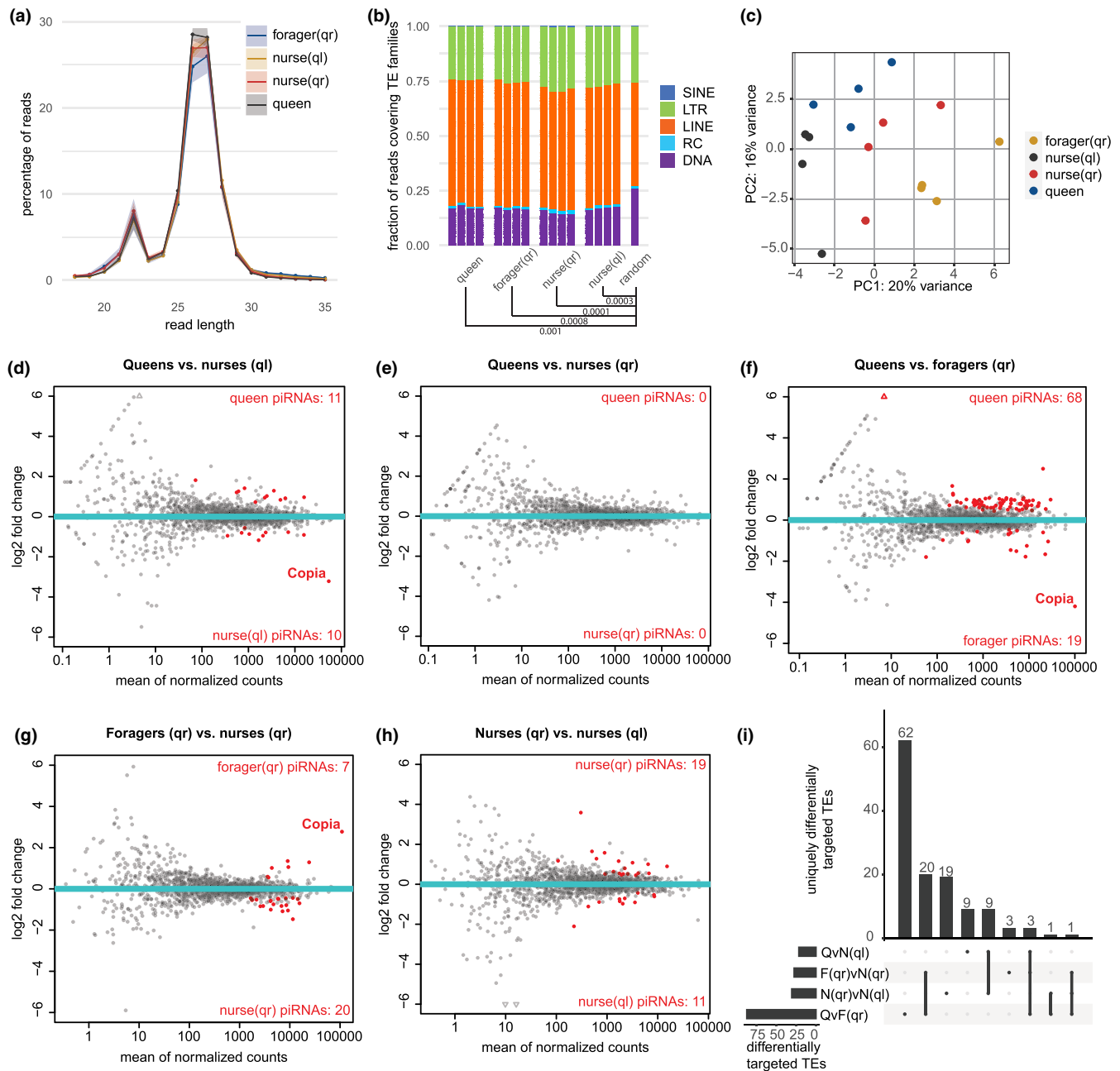


FIGURE 3 Ovarian piRNA expression in different castes. (a) Length distribution of all 18–35 nt ovarian reads generated by sRNA-Seq. Shaded areas depict standard deviation obtained from the four biological replicates. (b) Stacked bar plots showing piRNA-like reads (25–30 nt) attributed to different TE families. *t*-tests carried out for each TE family to find difference between each caste and annotation (random expectation). For each pair of comparisons, the lowest Holm-adjusted *p*-value is shown. All *p*-values are listed in the supplement. (c) Principal component (PC) analysis of piRNA-like reads (25–30 nt) that map to annotated TEs. (d–h) MA plots showing pairwise differential TE comparisons of piRNA targeting in the four castes. Each dot represents one TE type and red indicates significant changes (FDR < 0.05). All hits are reported in Table S2. (i) UpSet plot showing overlap of significantly differentially targeted TEs as defined in (d–h). Hits per comparison are shown in the horizontal bar plot, overlaps between comparisons are shown in the vertical bar plot. QvN(ql) = queens versus ql nurses, panel (d). F(qr)vN(qr) = foragers versus qr nurses, panel (g). N(qr)vN(ql) = qr nurses versus ql nurses, panel (h). QvF(qr) = queens versus foragers, panel (f).

species, where this has been seen to aid in AGO recognition and direction into the correct AGO (Seitz et al., 2011). In *D. melanogaster*, for instance, a uridine at the 5'-position will favour the uptake by the Argonaute AGO1 whereas a cytosine at the same position will favour uptake of the miRNA by AGO2 (Czech et al., 2009). In

mammals, AGO1 preferentially binds 5'-U and AGO-2 preferentially binds 5'-A (Frank et al., 2010).

Although relative miRNA expression was highest in the brain and thorax, ovaries expressed a more varied selection of miRNAs (Figure 4b). In the ovaries, we could detect the expression of 227

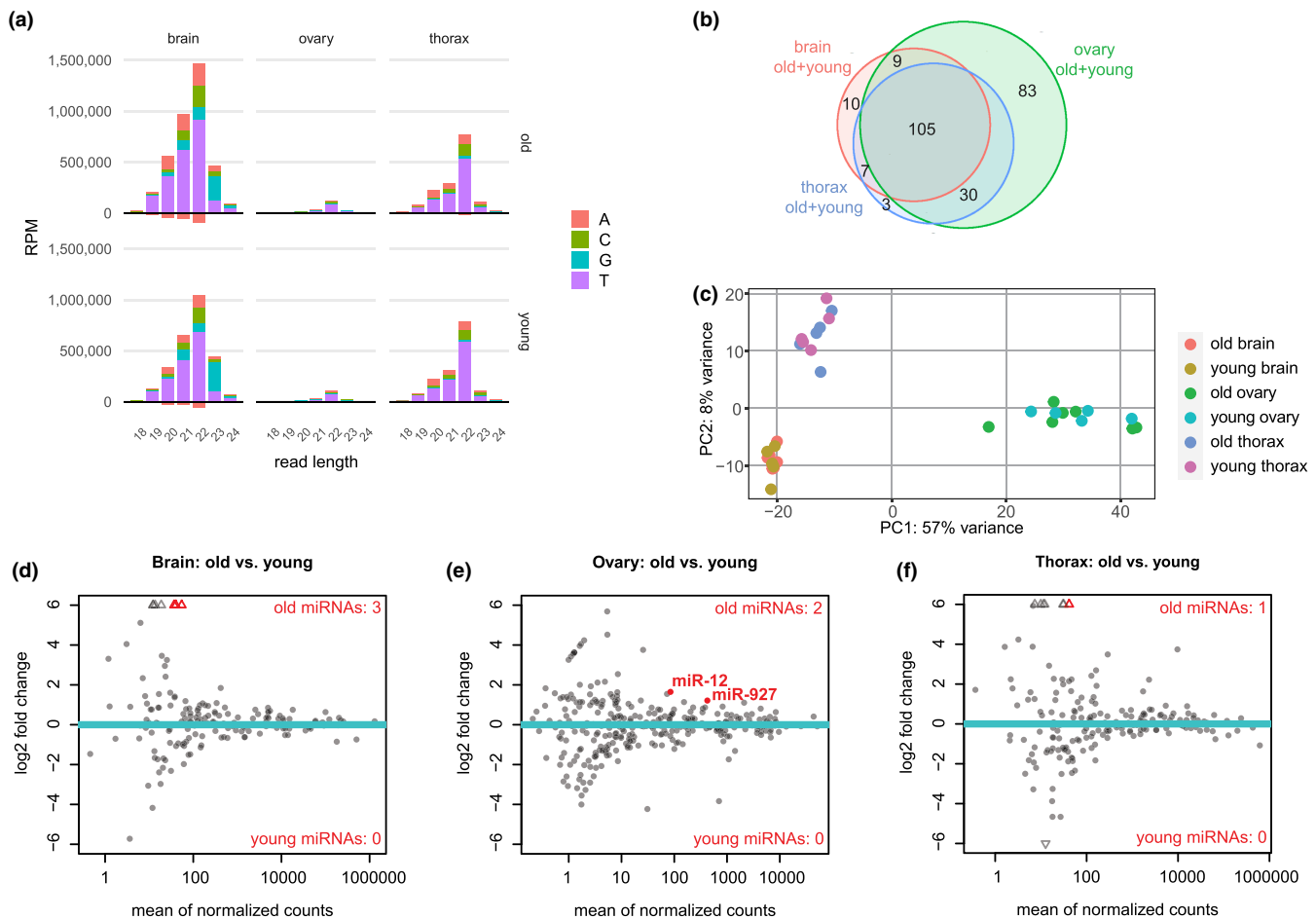


FIGURE 4 miRNA expression in different tissues of young- and middle-aged queens. (a) Length distribution of reads length 18–24 nt mapping sense (up) and antisense (down) to miRNAs. Values represent average of all five to seven replicates, colours represent the starting base. RPM, reads per million. (b) Venn diagram showing the overlap of distinct miRNAs found in at least three samples of brain, ovary and thorax. Old and young queens are pooled together. All miRNAs are listed in [Table S4](#). (c) Principal component analysis of miRNA reads. (d–f) MA plots showing pairwise differential expression comparisons of miRNAs in young versus older queens in the three tissues. Each dot represents one miRNA. Red indicates significant changes (FDR < 0.05). All hits are reported in [Table S5](#).

different miRNAs, 83 of which were unique for this tissue. In comparison, only 145 different miRNAs were detected in the thorax and 131 in the brain. We could detect 105 of the expressed miRNAs in all three tissues ([Figure 4b](#)). It is worth noting that expression here is defined as detection in at least three replicates of the same tissue, regardless of age, explaining why we find fewer expressed miRNAs (247 as shown in [Figure 4b](#)) than found in the genome (304, see above), where detection in three samples of *any* tissue was used as the filtering parameter. Altogether, we conclude that *T. rugatulus* does indeed express miRNAs and that these can be expressed tissue specifically.

3.8 | miRNA expression shifts only slightly with queen age

We next carried out differential analyses in order to detect miRNAs involved in ageing. Similar to the piRNAs, the major difference in miRNA expression was related to tissue type, not age

([Figure 4c](#)). In the thorax and brain, we could define one and three miRNAs that were upregulated in the middle-aged queens respectively. All of these were, however, lowly expressed ([Figure 4d–f](#)). In the ovaries, we found two miRNAs, miR-12 and miR-927a (both according to *A. mellifera* annotation), to be upregulated in middle-aged queens, although both showed modest change ([Figure 4e](#)). In general, miRNAs seemed to be only mildly affected by age in *T. rugatulus* queens.

3.9 | Ovarian miRNA expression is specific to caste and worker task

Finally, we investigated the ovarian miRNAs of queens, nurses from qr and ql colonies and foragers from qr colonies by isolating the reads in the range 18–24 nt and mapping these to our miRNA annotation. Similar to results in queens ([Figure 4a](#)), ovarian miRNAs of all groups mapped primarily sense to annotated miRNAs with a 5′-U bias ([Figure 5a](#)).

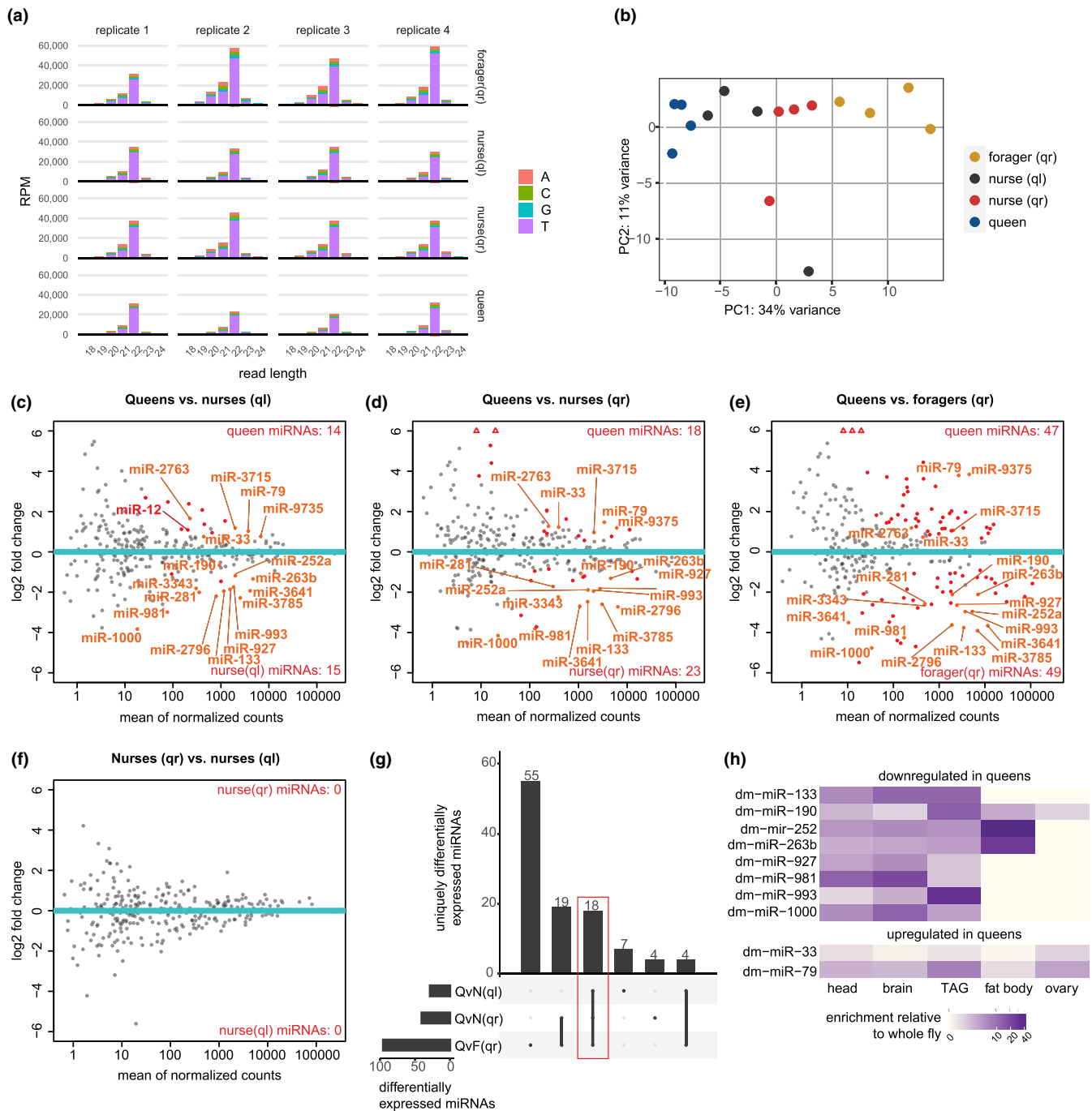


FIGURE 5 Ovarian miRNA expression in different castes. (a) Length distribution of ovarian reads length 18–24 nt mapping to miRNAs on sense (up) and antisense (down) strands. Colours represent the starting base. (b) Principal component (PC) analysis of miRNA reads. (c–f) MA plots showing pairwise differential expression comparisons of miRNAs in different castes. Each dot represents one miRNA. Named miRNAs are those indicated in the orange square in panel (g). Red indicates significant changes (FDR < 0.05). All hits are reported in Table S6. (g) UpSet plot showing overlap of significantly differentially expressed miRNAs as defined in (c–f). Hits per comparison are shown in the horizontal bar plot, overlaps between comparisons are shown in the vertical bar plot. QvN(ql) = queens versus ql nurses, panel (c). QvN(qr) = queens versus qr nurses, panel (d). QvF(qr) = queens versus foragers, panel (e). (h) Heatmap showing the relative expression of 10 miRNAs in *D. melanogaster* as reported in FlyAtlas2. These 10 miRNAs are those found in all comparisons (c–e) in five tissues (shown in the orange square in panel (g)) for which homologues exist in *D. melanogaster*. TAG, Thoracoabdominal ganglion.

We next overlapped our mapped miRNAs with the miRNA annotation that we had already generated using our first data set. In stark contrast to piRNAs, which showed little correlation between ovarian expression and group, we observed that miRNA expression

and ovarian activation state were highly associated. Principle component analysis revealed gradual shifts from active queen ovaries to activated ovaries of ql nurses, onward to inactive ovaries of qr nurses and the inactive ovaries of foragers (Figure 5b). Despite

this segregation of our samples, we could not identify any specific miRNAs that could be directly involved in the activation of ovaries, as we did not detect any significantly regulated miRNAs between nurses of ql and qr colonies (Figure 5f). However, we could define more than 100 miRNAs that were differentially expressed in different castes across all comparisons (Figure 5c–g, Table S6).

We wanted to investigate a subset of these miRNAs, and therefore decided to search FlyAtlas2 (Krause et al., 2022) for tissue-specific expression in *Drosophila melanogaster* of the 18 miRNAs that we found to be differentially expressed in queens in all three comparisons (queen vs. ql nurses, queen vs. qr nurses and queen vs. foragers). Two of the five miRNAs upregulated in queens and eight of the 13 miRNAs downregulated in queens had homologues with expression data in FlyAtlas2. We asked whether these miRNAs were generally known to be expressed in ovaries. Both of the queen-upregulated miRNAs are present in the *D. melanogaster* ovaries, but most of the queen-downregulated miRNAs did not show ovarian expression in *D. melanogaster* (Figure 5h). We noticed that all of the queen-downregulated miRNAs showed high expression in non-reproductive tissues; head, brain and the thoracoabdominal ganglion in *D. melanogaster* (Figure 5h). In other tissues such as the fat body, the expression level varied (Figure 5h). This indicates that non-queen ovary samples may carry significant amounts of other tissue(s). This could be due to their small size making them hard to dissect, or to the fact that these ovaries contain a lower fraction of germ cell mass, and hence relatively speaking more somatic tissue, or it could imply that these ovaries simply do express more miRNAs that are usually found in non-ovarian tissues.

We then compared the expression of specific miRNAs to studies on other social insects. We found miR-927a and miR-12 to be upregulated in the ovaries of middle-aged relative to young queens (Figure 4e) and miR-12 in addition upregulated in ovaries of queens relative to ql nurses (Figure 5c). In the honeybee *A. mellifera*, miR-927a and miR-12 were found to be overexpressed in virgin and inactive ovaries (Chen et al., 2017; Macedo et al., 2016). Indeed, we detected quite some overlap in differentially expressed miRNAs between the aforementioned honeybee studies and ours in ant ovaries, including miR-3049, miR-279b, miR-33, miR-190, miR-79 and miR-993. This points to ovarian miRNA expression being linked to ovarian development and female fecundity. Evidence for a conserved function of caste-specific expressed miRNAs comes from miR-133, which was universally downregulated in *T. rugatulus* queen ovaries compared to all worker samples (Figure 5c–e), and showed worker caste-specific expression in the termite *R. speratus* (Matsunami et al., 2018).

4 | DISCUSSION

4.1 | *T. rugatulus* expresses miRNAs and piRNAs

sRNA populations have been described in fungi, plants, invertebrates and mammals (Bartel, 2009; Ozata et al., 2019). In ants, sRNAs have so far only been described in the formicine *Camponotus floridanus*

and in the ponerine *Harpegnathos saltator* (Bonasio et al., 2010). Our study on the myrmicine *T. rugatulus* is thus the first on this subfamily of ants. We sampled *T. rugatulus* ants of different ages, castes and worker types and sequenced sRNAs from brain, thorax and ovaries in order to describe the expression landscape of sRNAs across these different groups.

Our analyses confidently show that the ant *T. rugatulus* expresses two distinct sRNA populations coinciding with piRNAs and miRNAs. We also demonstrate that the relative expression of piRNAs in *T. rugatulus* queens is higher in the ovaries than in somatic tissues, which is consistent with the general function of piRNAs in reproductive tissues, where TE surveillance is particularly important (Madhani, 2013) to reduce the risks of mutations in the germline.

4.2 | Only minor changes of piRNA expression exist between different castes of *T. rugatulus* ants

Our results indicate that piRNAs may also play a role in somatic tissues in ants, and particularly in the thorax (Figure 1). This is consistent with a previous report describing piRNAs in somatic tissues in several ancestral arthropod species (Lewis et al., 2018). We found divergent biases and different targets of piRNAs in queen brains, pointing to possibly alternate functions of these sRNAs in this tissue. In the termite *Macrotermes bellicosus*, TEs were found to be expressed in the heads of old workers but not in those of queens, which are much longer lived (Elsner et al., 2018). TEs were also much more active in the fat body of workers of the termite *M. natalensis* than in reproductive individuals (Post et al., 2023), leading to the prediction that pathway targeting TEs might be less active in non-reproductive individuals than in reproductive individuals. We demonstrated that the non-reproductive and regressed ovaries of nurses and foragers from queenright colonies not only have piRNAs at similar levels to those of queens, but also show ping-pong signatures and target TEs, all of which are features of an active TE-silencing piRNA pathway. We find that piRNAs are only slightly downregulated in foragers compared to queens (Figure 3a,f), but not nearly to the extent expected, as ovaries of foragers had regressed to the point where they were only translucent membranes. We therefore conclude that in *T. rugatulus*, reproductive and non-reproductive ovaries alike seem to have the capacity to silence TEs via piRNAs and this pathway is likely not linked to ovarian development. Rather, the high activity of piRNAs is a characteristic of ovarian tissue per se maintained even in old workers, despite them sometimes being regarded as the soma of the superorganism ant colony (Johnson & Linksvayer, 2010).

We detected 7–16 differentially targeted TEs between young- and middle-aged queens (Figure 1e–g). These had either a low sRNA levels overall, as in the brain and thorax, or were strongly expressed but only weakly differentially regulated, as in the ovaries, the tissue that showed the most pronounced differences. The weak differences could indicate that piRNAs and miRNAs—we also found only minor differences in those regulatory RNAs—do

not play a major role in physiological ageing in this species. The minor shifts in sRNAs could also be due to slow ageing in *T. rugatulus* queens. Although *Temnothorax* queens can live up to 20 years (Plateaux, 1986), our study compared queens with an age of half a year and more than 4 years and probably did not include senescent queens at the end of their life. Moreover, the young- and middle-aged queens in our study showed no differences in ovarian development, which distinguished them from those in a previous gene expression study in which the young queens had significantly less developed ovaries and also showed strong transcriptional differences in the fat body (Negroni et al., 2019). In the ant species *Cardiocondyla obscurior*, there were also only minor expression changes between young- and middle-aged queens, which indicated a stable physiology over a long period of time (von Wychetzkki et al., 2015), but dramatic changes at the very end of life indicative of rapid physiological degeneration (Jaimes-Nino et al., 2022). Therefore, it is conceivable that the minimal change in sRNAs with queen age in our study indicates slowed ageing in the young- to middle-aged queens of our model *T. rugatulus*.

4.3 | miRNA expression in relation to ageing and ovarian activation state

We detected 304 miRNAs in *T. rugatulus*, which is about double to triple the number annotated in the genomes of *H. saltator* (159) and in *C. floridanus* (96) (Bonasio et al., 2010). Nevertheless, many of our miRNAs are clear homologues of known miRNAs. Some of them are broadly expressed, but we also detected tissue-specific expression. We found only six miRNAs that were differentially expressed between young- and middle-aged queens in the tissues analysed (Figure 4d–f), and these either differed only slightly in expression or were expressed at very low levels. One miRNA upregulated in the ovaries of older queens, miR-12, was also found to be upregulated in active ovaries of queens relative to nurses from queenless colonies (Figure 5c). Interestingly, in *A. mellifera* (Macedo et al., 2016), miR-12 is predominantly expressed in inactive ovaries of virgin queens, suggesting that miR-12 and possibly also miR-927a have a conserved role linked to ovarian activity, but may have different target genes in *A. mellifera* compared to *T. rugatulus*. Overall, our data suggest that miRNAs are rather stably expressed in queens over many years in *T. rugatulus*, suggesting little changes in molecular physiology with age. In contrast, we discovered very large differences in miRNA populations between the ovaries of queens and workers. Indeed, 96 miRNAs were different in expression between queens and foragers (Figure 5c–e). The latter represent the oldest worker generation (Kohlmeier et al., 2019) with most regressed ovaries. In contrast, only a quarter to half as many miRNAs were differentially between queens and nurses from queenless (25) and queenright (41) colonies. These younger workers mostly exhibit extended ovaries with developing eggs. Also, the principal component analysis based on all miRNAs does not show a dichotomy between queens and workers, but rather a gradual shift with queen samples

at one end and forager samples at the other end and nurses in the middle, suggesting a possible correlation between miRNA expression profiles and ovarian activation (Figure 5b). Several miRNAs were differentially expressed in individual comparisons between the reproductive ovaries of queens, and less activated ovaries of nurses or foragers. We found no miRNAs to be differentially expressed between nurses from either queenright or queenless colonies (Figure 5f), which might be due to the fact that the number of eggs and ovarian development between these two groups was insignificant in our study (Figure 2c,e), albeit earlier studies showing that queen removal can cause changes in fat body gene expression linked to reproductive state (Choppin et al., 2021; Negroni et al., 2020, 2021). As more social insects have their miRNA profiles mapped, it will in the future become possible to do a more in-depth comparison and determine conserved versus species-specific caste-associated miRNAs and possibly to elucidate the evolutionary mechanisms behind the roles of specific sRNAs in the complex lifestyles of social insects. Based on our findings, we hypothesise that miRNAs in the ovaries play an important role in regulating fertility in ants and do not solely reflect caste status.

AUTHOR CONTRIBUTIONS

Susanne Foitzik and René Ketting designed the study. Marina Choppin, Barbara Feldmeyer and Susanne Foitzik collected the ant colonies. Marina Choppin, Marion Kever and Susanne Foitzik dissected the ants, measured the ovaries and prepared the samples. The TE annotation was done by Alice Séguret. The RNA was extracted by Marion Kever, Ann-Sophie Seistrup and Shamitha Govind, the latter two also performing all other molecular biology work in the lab. The miRNA annotation and bioinformatic analyses were performed by Emil Karaulanov, Sivarajan Karunanithi, Miguel V. Almeida, Ann-Sophie Seistrup and Shamitha Govind. Data analysis and manuscript preparation were carried out by Ann-Sophie Seistrup, René Ketting and Susanne Foitzik with the support of all co-authors.

ACKNOWLEDGEMENTS

This project was funded by the Deutsche Forschungsgemeinschaft (DFG, German Research Foundation)—GRK2526/1—Projectnr. 407023052 and FO 298/19–2 within the research unit FOR-2281. Support by the IMB Genomics Core Facility and the use of its NextSeq500 (funded by DFG—INST 247/870-1 FUGG) is gratefully acknowledged. Open Access funding enabled and organized by Projekt DEAL.

CONFLICT OF INTEREST STATEMENT

The authors report no conflict of interest.

DATA AVAILABILITY STATEMENT

Raw sequence data were deposited in the NCBI Sequence Read Archive (SRA) under BioProject PRJNA955004. Draft genome was provided by Jongepier et al. (2022), available under BioProject PRJNA750352 and TE annotation can be found in supplementary data (TE_annotation_trug.fa.out.gz) respectively.

ORCID

Barbara Feldmeyer  <https://orcid.org/0000-0002-0413-7245>Susanne Foitzik  <https://orcid.org/0000-0001-8161-6306>

REFERENCES

- Andrews, S. (2010). FASTQC. A quality control tool for high throughput sequence data.
- Bartel, D. P. (2009). MicroRNAs: Target recognition and regulatory functions. *Cell*, 136(2), 215–233. <https://doi.org/10.1016/j.cell.2009.01.002>
- Behura, S. K., & Whitfield, C. W. (2010). Correlated expression patterns of microRNA genes with age-dependent behavioural changes in honeybee. *Insect Molecular Biology*, 19(4), 431–439. <https://doi.org/10.1111/j.1365-2583.2010.01010.x>
- Bohn, J., Halabian, R., Schrader, L., Shabardina, V., Steffen, R., Suzuki, Y., Ernst, U. R., Gadau, J., & Makiowski, W. (2021). Genome assembly and annotation of the California harvester ant *Pogonomyrmex californicus*. *G3 Genes[Genomes]Genetics*, 11(1), jkaa019. <https://doi.org/10.1093/g3journal/jkaa019>
- Bonasio, R., Zhang, G., Ye, C., Mutti, N. S., Fang, X., Qin, N., Donahue, G., Yang, P., Li, Q., Li, C., Zhang, P., Huang, Z., Berger, S. L., Reinberg, D., Wang, J., & Liebig, J. (2010). Genomic comparison of the ants *Camponotus floridanus* and *Harpegnathos saltator*. *Science*, 329(5995), 1068–1071. <https://doi.org/10.1126/science.1192428>
- Boomsma, J. J., & Gawne, R. (2018). Superorganismality and caste differentiation as points of no return: How the major evolutionary transitions were lost in translation. *Biological Reviews*, 93(1), 28–54. <https://doi.org/10.1111/brv.12330>
- Bourke, A. F. G. (1988). Worker reproduction in the higher eusocial hymenoptera. *The Quarterly Review of Biology*, 63(3), 291–311. <https://doi.org/10.1086/415930>
- Brennecke, J., Aravin, A. A., Stark, A., Dus, M., Kellis, M., Sachidanandam, R., & Hannon, G. J. (2007). Discrete small RNA-generating loci as master regulators of transposon activity in *Drosophila*. *Cell*, 128(6), 1089–1103. <https://doi.org/10.1016/j.cell.2007.01.043>
- Chen, H., & Boutros, P. C. (2011). VennDiagram: A package for the generation of highly-customizable Venn and Euler diagrams in R. *BMC Bioinformatics*, 12(1), 35. <https://doi.org/10.1186/1471-2105-12-35>
- Chen, X., Ma, C., Chen, C., Lu, Q., Shi, W., Liu, Z., Wang, H., & Guo, H. (2017). Integration of lncRNA-miRNA-mRNA reveals novel insights into oviposition regulation in honey bees. *PeerJ*, 5, e3881. <https://doi.org/10.7717/peerj.3881>
- Choppin, M., Feldmeyer, B., & Foitzik, S. (2021). Histone acetylation regulates the expression of genes involved in worker reproduction in the ant *Temnothorax rugatulus*. *BMC Genomics*, 22, 871. <https://doi.org/10.1186/s12864-021-08196-8>
- Coenen-Stass, A. M. L., Sork, H., Gatto, S., Godfrey, C., Bhomra, A., Krjutškov, K., Hart, J. R., Westholm, J. O., O'Donovan, L., Roos, A., Lochmüller, H., Puri, P. L., El Andaloussi, S., Wood, M. J. A., & Roberts, T. C. (2018). Comprehensive RNA-sequencing analysis in serum and muscle reveals novel small RNA signatures with biomarker potential for DMD. *Molecular Therapy - Nucleic Acids*, 13, 1–15. <https://doi.org/10.1016/j.omtn.2018.08.005>
- Conway, J. R., Lex, A., & Gehlenborg, N. (2017). UpSetR: An R package for the visualization of intersecting sets and their properties. *Bioinformatics*, 33(18), 2938–2940. <https://doi.org/10.1093/bioinformatics/btx364>
- Corona, M., Libbrecht, R., & Wheeler, D. E. (2016). Molecular mechanisms of phenotypic plasticity in social insects. *Current Opinion in Insect Science*, 13, 55–60. <https://doi.org/10.1016/j.cois.2015.12.003>
- Czech, B., Zhou, R., Erlich, Y., Brennecke, J., Binari, R., Villalta, C., Gordon, A., Perrimon, N., & Hannon, G. J. (2009). Hierarchical rules for Argonaute loading in *Drosophila*. *Molecular Cell*, 36(3), 445–456. <https://doi.org/10.1016/j.molcel.2009.09.028>
- Danecek, P., Bonfield, J. K., Liddle, J., Marshall, J., Ohan, V., Pollard, M. O., Whitwham, A., Keane, T., McCarthy, S. A., Davies, R. M., & Li, H. (2021). Twelve years of SAMtools and BCFtools. *GigaScience*, 10(2), giab008. <https://doi.org/10.1093/gigascience/giab008>
- Elsik, C. G., Worley, K. C., Bennett, A. K., et al. (2014). Finding the missing honey bee genes: lessons learned from a genome upgrade. *BMC Genomics*, 15, 86. <https://doi.org/10.1186/1471-2164-15-86>
- Elsner, D., Meusemann, K., & Korb, J. (2018). Longevity and transposon defense, the case of termite reproductives. *Proceedings of the National Academy of Sciences*, 115(21), 5504–5509. <https://doi.org/10.1073/pnas.1804046115>
- Ender, C., & Meister, G. (2010). Argonaute proteins at a glance. *Journal of Cell Science*, 123(11), 1819–1823. <https://doi.org/10.1242/jcs.055210>
- Faulk, C. (2023). De novo sequencing, diploid assembly, and annotation of the black carpenter ant, *Camponotus pennsylvanicus*, and its symbionts by one person for \$1000, using nanopore sequencing. *Nucleic Acids Research*, 51(1), 17–28. <https://doi.org/10.1093/nar/gkac510>
- Filipowicz, W., Bhattacharyya, S. N., & Sonenberg, N. (2008). Mechanisms of post-transcriptional regulation by microRNAs: Are the answers in sight? *Nature Reviews. Genetics*, 9(2), 102–114. <https://doi.org/10.1038/nrg2290>
- Flatt, T. (2011). Survival costs of reproduction in *Drosophila*. *Experimental Gerontology*, 46(5), 369–375. <https://doi.org/10.1016/j.exger.2010.10.008>
- Frank, F., Sonenberg, N., & Nagar, B. (2010). Structural basis for 5'-nucleotide base-specific recognition of guide RNA by human AGO2. *Nature*, 465(7299), 818–822. <https://doi.org/10.1038/nature09039>
- Friedländer, M. R., Mackowiak, S. D., Li, N., Chen, W., & Rajewsky, N. (2012). miRDeep2 accurately identifies known and hundreds of novel microRNA genes in seven animal clades. *Nucleic Acids Research*, 40(1), 37–52. <https://doi.org/10.1093/nar/gkr688>
- Gilbert, C., Peccoud, J., & Cordaux, R. (2021). Transposable Elements and the Evolution of Insects. *Annual Review of Entomology*, 66(1), 355–372.
- Griffiths-Jones, S., Bateman, A., Marshall, M., Khanna, A., & Eddy, S. R. (2003). Rfam: An RNA family database. *Nucleic Acids Research*, 31(1), 439–441. <https://doi.org/10.1093/nar/gkg006>
- Heinze, J., & Schrepf, A. (2012). Terminal investment: Individual reproduction of ant queens increases with age. *PLoS One*, 7(4), e35201. <https://doi.org/10.1371/journal.pone.0035201>
- Hirano, T., Iwasaki, Y. W., Lin, Z. Y., Imamura, M., Seki, N. M., Sasaki, E., Saito, K., Okano, H., Siomi, M. C., & Siomi, H. (2014). Small RNA profiling and characterization of piRNA clusters in the adult testes of the common marmoset, a model primate. *RNA*, 20(8), 1223–1237. <https://doi.org/10.1261/rna.045310.114>
- Jaimes-Nino, L. M., Heinze, J., & Oettler, J. (2022). Late-life fitness gains and reproductive death in *Cardiophila obscurior* ants. *eLife*, 11, e74695. <https://doi.org/10.7554/eLife.74695>
- Johnson, B. R., & Linksvayer, T. A. (2010). Deconstructing the superorganism: Social physiology, Groundplans, and Sociogenomics. *The Quarterly Review of Biology*, 85(1), 57–79. <https://doi.org/10.1086/650290>
- Jongepier, E., Séguret, A., Labutin, A., Feldmeyer, B., Gstöttl, C., Foitzik, S., Heinze, J., & Bornberg-Bauer, E. (2022). Convergent loss of chemoreceptors across independent origins of slave-making in ants. *Molecular Biology and Evolution*, 39(1), msab305. <https://doi.org/10.1093/molbev/msab305>
- Kapheim, K. M., Jones, B. M., Søvik, E., Stolle, E., Waterhouse, R. M., Bloch, G., & Ben-Shahar, Y. (2020). Brain microRNAs among social and solitary bees. *Royal Society Open Science*, 7(7), 200517. <https://doi.org/10.1098/rsos.200517>

- Keller, L., & Genoud, M. (1997). Extraordinary lifespans in ants: A test of evolutionary theories of ageing. *Nature*, 389(6654), 958–960. <https://doi.org/10.1038/40130>
- Ketting, R. F., & Cochella, L. (2021). Concepts and functions of small RNA pathways in *C. Elegans*. *Current Topics in Developmental Biology*, 144, 45–89. <https://doi.org/10.1016/bs.ctdb.2020.08.002>
- Kinsler, H. E., & Pincus, Z. (2020). MicroRNAs as modulators of longevity and the aging process. *Human Genetics*, 139(3), 291–308. <https://doi.org/10.1007/s00439-019-02046-0>
- Kohlmeier, P., Alleman, A. R., Libbrecht, R., Foitzik, S., & Feldmeyer, B. (2019). Gene expression is more strongly associated with behavioural specialization than with age or fertility in ant workers. *Molecular Ecology*, 28(3), 658–670. <https://doi.org/10.1111/mec.14971>
- Krause, S. A., Overend, G., Dow, J. A. T., & Leader, D. P. (2022). FlyAtlas 2 in 2022: Enhancements to the *Drosophila melanogaster* expression atlas. *Nucleic Acids Research*, 50(D1), D1010–D1015. <https://doi.org/10.1093/nar/gkab971>
- Langmead, B., Trapnell, C., Pop, M., & Salzberg, S. L. (2009). Ultrafast and memory-efficient alignment of short DNA sequences to the human genome. *Genome Biology*, 10(3), R25. <https://doi.org/10.1186/gb-2009-10-3-r25>
- Lewis, B. P., Shih, I. H., Jones-Rhoades, M. W., Bartel, D. P., & Burge, C. B. (2003). Prediction of mammalian microRNA targets. *Cell*, 115(7), 787–798. [https://doi.org/10.1016/s0092-8674\(03\)01018-3](https://doi.org/10.1016/s0092-8674(03)01018-3)
- Lewis, S. H., Quarles, K. A., Yang, Y., Tanguy, M., Frézal, L., Smith, S. A., Shirma, P. P., Cordaux, R., Gilbert, C., Giraud, I., Collins, D. H., Zamore, P. D., Miska, E. A., Sarkies, P., & Jiggins, F. M. (2018). Panarthropod analysis reveals somatic piRNAs as an ancestral defence against transposable elements. *Nature Ecology & Evolution*, 2(1), 174–181. <https://doi.org/10.1038/s41559-017-0403-4>
- Liao, Y., Smyth, G. K., & Shi, W. (2013). The subread aligner: Fast, accurate and scalable read mapping by seed-and-vote. *Nucleic Acids Research*, 41(10), e108. <https://doi.org/10.1093/nar/gkt214>
- Love, M. I., Huber, W., & Anders, S. (2014). Moderated estimation of fold change and dispersion for RNA-seq data with DESeq2. *Genome Biology*, 15(12), 550. <https://doi.org/10.1186/s13059-014-0550-8>
- Ludwig, N., Becker, M., Schumann, T., Speer, T., Fehlmann, T., Keller, A., & Meese, E. (2017). Bias in recent miRBase annotations potentially associated with RNA quality issues. *Scientific Reports*, 7(1), 5162. <https://doi.org/10.1038/s41598-017-05070-0>
- Luo, S., & Lu, J. (2017). Silencing of transposable elements by piRNAs in *drosophila*: An evolutionary perspective. *Genomics, Proteomics & Bioinformatics*, 15, 164–176. <https://doi.org/10.1016/j.gpb.2017.01.006>
- Macedo, L. M., Nunes, F. M., Freitas, F. C., Pires, C. V., Tanaka, E. D., Martins, J. R., Plulachs, M. D., Cristino, A. S., Pinheiro, D. G., & Simões, Z. L. (2016). MicroRNA signatures characterizing caste-independent ovarian activity in queen and worker honeybees (*Apis mellifera* L.). *Insect Molecular Biology*, 25(3), 216–226. <https://doi.org/10.1111/imb.12214>
- Madhani, H. D. (2013). The frustrated gene: Origins of eukaryotic gene expression. *Cell*, 155(4), 744–749. <https://doi.org/10.1016/j.cell.2013.10.003>
- Maklakov, A. A., & Chapman, T. (2019). Evolution of ageing as a tangle of trade-offs: Energy versus function. *Proceedings of the Royal Society B: Biological Sciences*, 286(1911), 20191604. <https://doi.org/10.1098/rspb.2019.1604>
- Martin, M. (2011). Cutadapt removes adapter sequences from high-throughput sequencing reads. *EMBnet Journal*, 17(1), 3. [doi:10.14806/ej.17.1.200](https://doi.org/10.14806/ej.17.1.200)
- Matsunami, M., Nozawa, M., Suzuki, R., Toga, K., Masuoka, Y., Yamaguchi, K., Maekawa, K., Shigenobu, S., & Miura, T. (2018). Caste-specific microRNA expression in termites: Insights into soldier differentiation. *Insect Molecular Biology*, 28(1), 86–98. <https://doi.org/10.1111/imb.12530>
- Negrone, M. A., Foitzik, S., & Feldmeyer, B. (2019). Long-lived *Temnothorax* ant queens switch from investment in immunity to antioxidant production with age. *Scientific Reports*, 9(1), 7270. <https://doi.org/10.1038/s41598-019-43796-1>
- Negrone, M. A., Macit, M. N., Stoldt, M., Feldmeyer, B., & Foitzik, S. (2021). Molecular regulation of lifespan extension in fertile ant workers. *Philosophical Transactions of the Royal Society B: Biological Sciences*, 376(1823), 20190736. <https://doi.org/10.1098/rstb.2019.0736>
- Negrone, M. A., Segers, F. H. I. D., Vogelweith, F., & Foitzik, S. (2020). Immune challenge reduces gut microbial diversity and triggers fertility-dependent gene expression changes in a social insect. *BMC Genomics*, 21(1), 816. <https://doi.org/10.1186/s12864-020-07191-9>
- Nouhaud, P., Beresford, J., & Kulmuni, J. (2022). Assembly of a hybrid *Formica aquilonia* × *F. Polyctena* ant genome from a haploid male. *Journal of Heredity*, 113(3), 353–359. <https://doi.org/10.1093/jhered/esac019>
- Ozata, D. M., Gainetdinov, I., Zoch, A., O'Carroll, D., & Zamore, P. D. (2019). PIWI-interacting RNAs: Small RNAs with big functions. *Nature Reviews. Genetics*, 20(2), 89–108. <https://doi.org/10.1038/s41576-018-0073-3>
- Plateaux, L. (1986). Comparaison des cycles saisonniers, des durées des sociétés et des productions des trois espèces de fourmis *Leptothorax* (Myrmecinae) du groupe nylanderii. *Actes Des Colloques Insectes Sociaux*, 3, 221–234.
- Post, F., Bornberg-Bauer, E., Vasseur-Cognet, M., & Harrison, M. C. (2023). More effective transposon regulation in fertile, long-lived termite queens than in sterile workers. *Molecular Ecology*, 32(2), 369–380. <https://doi.org/10.1111/mec.16753>
- Quinlan, A. R., & Hall, I. M. (2010). BEDTools: A flexible suite of utilities for comparing genomic features. *Bioinformatics*, 26(6), 841–842. <https://doi.org/10.1093/bioinformatics/btq033>
- R Core Team. (2013). *R: A language and environment for statistical computing*. R Foundation for Statistical Computing. <http://www.R-project.org/>
- Ramírez, F., Ryan, D. P., Grüning, B., Bhardwaj, V., Kilpert, F., Richter, A. S., Heyne, S., Dünder, F., & Manke, T. (2016). deepTools2: A next generation web server for deep-sequencing data analysis. *Nucleic Acids Research*, 44(W1), W160–W165. <https://doi.org/10.1093/nar/gkw257>
- Seitz, H., Tushir, J. S., & Zamore, P. D. (2011). A 5'-uridine amplifies miRNA/miRNA* asymmetry in *drosophila* by promoting RNA-induced silencing complex formation. *Silence*, 2, 4. <https://doi.org/10.1186/1758-907x-2-4>
- Smit, A. F. A., Hubley, R., & Green, P. (2013–2015). RepeatMasker Open-4.0. <http://www.repeatmasker.org>
- Sturm, Á., Perczel, A., Ivics, Z., & Vellai, T. (2017). The Piwi-piRNA pathway: Road to immortality. *Ageing Cell*, 16(5), 906–911. <https://doi.org/10.1111/accel.12630>
- Szathmáry, E., & Smith, J. M. (1995). The major evolutionary transitions. *Nature*, 374(6519), 227–232. <https://doi.org/10.1038/374227a0>
- Uhrig, S., & Klein, H. (2019). PingPongPro: A tool for the detection of piRNA-mediated transposon-silencing in small RNA-Seq data. *Bioinformatics*, 35(2), 335–336. <https://doi.org/10.1093/bioinformatics/bty578>
- von Wyszczetki, K., Rueppell, O., Oettler, J., & Heinze, J. (2015). Transcriptomic Signatures Mirror the Lack of the Fecundity/Longevity Trade-Off in Ant Queens. *Molecular Biology and Evolution*, 32(12), 3173–3185. <https://doi.org/10.1093/molbev/msv186>
- Wang, W., Ashby, R., Ying, H., Maleszka, R., & Forêt, S. (2017). Contrasting sex- and caste-dependent piRNA profiles in the transposon depleted Haplodiploid honeybee *Apis mellifera*. *Genome Biology and Evolution*, 9(5), 1341–1356. <https://doi.org/10.1093/gbe/evx087>
- Wheeler, W. M. (1911). The ant-colony as an organism. *Journal of Morphology*, 22(2), 307–325. <https://doi.org/10.1002/jmor.1050220206>
- Wickham, H. (2016). *ggplot2: Elegant graphics for data analysis*. Springer-Verlag.

- Zerbino, D. R., Johnson, N., Juettemann, T., Wilder, S. P., & Flicek, P. (2014). WiggleTools: Parallel processing of large collections of genome-wide datasets for visualization and statistical analysis. *Bioinformatics*, 30(7), 1008–1009. <https://doi.org/10.1093/bioinformatics/btt737>
- Zhang, J., Chen, S., & Liu, K. (2022). Structural insights into piRNA biogenesis. *Biochim Biophys Acta Gene Regul Mech*, 1865(2), 194799. <https://doi.org/10.1016/j.bbagr.2022.194799>

SUPPORTING INFORMATION

Additional supporting information can be found online in the Supporting Information section at the end of this article.

How to cite this article: Seistrup, A.-S., Choppin, M., Govind, S., Feldmeyer, B., Kever, M., Karaulanov, E., Séguret, A., Karunanithi, S., Almeida, M. V., Ketting, R. F., & Foitzik, S. (2023). Age- and caste-independent piRNAs in the germline and miRNA profiles linked to caste and fecundity in the ant *Temnothorax rugatulus*. *Molecular Ecology*, 32, 6027–6043. <https://doi.org/10.1111/mec.17162>